Localized Functionalization of Individual Colloidal Carriers for Cell Targeting and Imaging

Allison M. Yake, Alisar S. Zahr, Huda A. Jerri, Michael V. Pishko,* and Darrell Velegol*

Department of Chemical Engineering, The Pennsylvania State University, University Park, Pennsylvania 16802

Received January 19, 2007; Revised Manuscript Received March 9, 2007

Fabricating drug particles for therapeutic delivery and imaging presents important challenges in the design of the particle surfaces. Drug nanoparticle surfaces are currently functionalized with site-specific targeting ligands, biocompatible polymers, or fluorophore−polymer conjugates for specific imaging. However, if these functionalizations were to be synthesized on the drug carrier in localized, nanoscale regions on the particle surface, new schemes of drug delivery could be realized. Here we describe the use of our particle lithography technique that enables the synthesis of individual colloidal carrier assemblies that can be imaged and targeted to integrin-expressing cells. We show localized adhesion specificity for cells expressing the target integrin followed by receptor-mediated endocytosis. With the addition of localized delivery by adding drug nanoparticles to a specific region on the particle surface, our colloidal carrier assemblies have the potential to target, deliver therapeutic agents to, sense, and image diseased endothelium.

Introduction

Polymeric drug delivery systems are critical in the treatment of cancer, genetic diseases, and other life-threatening ailments.[1,2] The demand for drug delivery systems in the United States is projected to grow approximately 9% annually, exceeding profits of $82 billion by 2007.[3] The development of targeted and controlled release drug delivery systems is essential for the treatment and prevention of life-threatening diseases like cancer.[4,5] Effective treatment of cancer currently involves the use of highly toxic chemotherapeutic agents that destroy both tumorous and healthy cells in the body. In order to decrease the systemic toxicity and improve treatment efficacy, targeted drug assemblies need to be able to treat only the unhealthy cells through specific adhesion and controlled release and ensure that the healthy cells are spared.[5,6] A multifunctional surface with the ability to specifically target, deliver therapeutic agents, and diagnostically image diseased tissue in real time is an unmet medical need and would be a significant development in drug delivery research.[7−9]

Particles that are surface-modified with ligands have the ability to target their receptors that are expressed on the surface of cells. Angiogenesis, defined as the formation of new blood vessels that is enhanced in tumor growth, has been shown to be an important factor in tumor growth and metastasis.[10,11] Tumor growth cannot proceed without the development of a supportive vascular network.[12] Thus, intensive research into therapeutic approaches[12] that directly target the tumor vasculature to decrease or eliminate metastasis activity have received much attention. This is particularly relevant due to recent studies that have shown stem cells being implicated in maintaining certain cancers.[13] Tumor vasculature targeting has many potential advantages such as easy access to target ligands expressed by the "activated" endothelium, selectivity to tumor endothelium that may decrease systemic toxicity, capability of synergistic combination with anti-tumor agents, and the broad applicability of antiangiogenic therapy.[14] One interesting antiangiogenic approach is to target integrin receptors that are expressed on the surface of the tumor vasculature and to regulate cell growth during angiogenesis. The activated endothelium in angiogenic vessels within solid tumors overexpresses proteins such as vascular endothelial growth factor (VEGF), matrix metalloproteinases 2 and 9 (MMP-2 and MMP-9), adhesion molecule integrin $\alpha_v\beta_3$, and E-cadherin.[15] The $\alpha_v\beta_3$ integrin is more profoundly expressed on tumor cells and on tumor vasculature endothelial cells but is not typically found on blood vessels or normal healthy tissues.[12] In addition, the $\alpha_v\beta_3$ integrin is a receptor specific for the arginine-glycine-aspartic acid (RGD) peptide sequence. Short peptides that contain this RGD sequence have the ability to mimic cell adhesion molecules and bind to the $\alpha_v\beta_3$ integrin.[10,12,16−18] Thus, particles that are surface-modified with the RGD sequence may be used to target tumor endothelium.

We have the ability to merge nano- and microtechnologies that are critical to the engineering of drug delivery particles of the correct size and shape and with surface properties to promote uptake in desired regions. This has been demonstrated by the development of a multifunctional imaging particle that is capable of targeting specific cells, and which in the future will deliver essential treatment drugs in a focused manner. The synthesis is accomplished by combining layer-by-layer encapsulation of colloidal imaging particles[19−22] with the "particle lithography" technique[23] for patterning colloidal surfaces in designed ways. The imaging particles have been site-specifically modified by application of the "particle lithography" technique so that, for example, a controlled small area of the carrier particle is covalently bound to RGD peptide targeting agents that specifically adhere to integrins on the surface of fibroblast cells. [Note: We differentiate the term site-specific from its drug delivery context, such that we use the term site-specific to designate a particular surface location on a single colloidal particle.] Fluorescent polystyrene latex nanoparticles, used as an inexpensive model for drug nanoparticles, were then selectively

* To whom correspondence should be addressed: (M.V.P.) phone (814) 863-4810, e-mail mpishko@engr.psu.edu; (D.V.) phone (814) 865-8739, e-mail velegol@psu.edu.

10.1021/bm070071r CCC: $37.00
Published on Web 05/04/2007

adhered to predetermined regions on the imaging particles. We have the ability to further adapt the system for better biocompatibility by modifying the surface of the multifunctional drug assemblies to overcome rejection and uptake by the body. In addition, we can use drug nanoparticles placed in a localized region on the surface of the colloidal carrier particle to allow for controlled release of the drug into the affected region of the body.

The key advance of this technology is our ability to synthesize multiple functions in particular nanoscale regions on the surfaces of individual colloidal particles. This type of more specific and selective targeting scheme, with the addition of locally placed drug nanoparticles on the assembly, may reduce undesirable side effects by killing the tumorous cells and not all similar cells within the body. Due to the specific nature of the delivery mechanism, the treatment may result in less overall systemic toxicity than conventional chemotherapy, lower the risk of improper dosing, improve life expectancy, and improve the quality of the patient's life during and after treatments.

Experimental Section

Materials. Monodisperse, surfactant-free sulfate-functionalized fluorescent polystyrene latex (PSL) microspheres were purchased from Interfacial Dynamics Corp. (Portland, OR). Specifically, 60 nm sulfate-functionalized fluorescent yellow-green PSL (batch 1-FLY-60.1), 43 nm sulfate-functionalized PSL (batch 2012,1), 84 nm sulfate-functionalized PSL (batch 124,1), 190 nm sulfate-functionalized fluorescent yellow-green PSL (batch 1-FLY-200.1), 200 nm carboxyl-functionalized fluorescent orange PSL (batch F-8809) and 4.0 μm sulfate-functionalized fluorescent nile red (batch 1-FLN-4K.2) and fluorescent yellow-green (batch 1-FLY-4K.2) PSL microspheres were used in the experiments described in this paper. Monodisperse, 3.0 μm silica microspheres (lot F300) were purchased from the Corpuscular Company (Mahopac, NY). Potassium chloride (KCl, MW 74.5), sodium chloride (NaCl, MW 58.4), potassium dihydrogen phosphate (KH_2PO_4, MW 136.1), dibasic sodium phosphate (Na_2HPO_4, MW 141.9), poly(allylamine hydrochloride) (PAH, MW 70 000), poly(sodium 4-styrenesulfonate) (PSS, MW 70 000), 1-ethyl-3-(3-dimethylaminopropyl)-carbodiimide (EDC, MW 191.7), 2-(*N*-morpholino)ethanesulfonic acid (MES, MW 195.2, pH 6.2), 2-mercaptoethanol, dimethyl sulfoxide (DMSO, MW 78.1), and *N*-hydroxysuccinimide (NHS, MW 115.1) were purchased from Sigma−Aldrich. Gly-Arg-Ala-Asp-Ser-Pro (GRADSP, lot S07075A1, 44-0-21) and Gly-Arg-Gly-Asp-Ser-Pro (GRGDSP, lot S07043A1, 44-0-24) peptide complexes were purchased from American Peptide Co., Inc. (Vista, CA).

Dulbecco's modified Eagle's medium (DMEM) and antibiotic−antimycotic were purchased from Sigma. Fetal bovine serum (FBS) was purchased from Hyclone. Flasks for cell culture, T-75 and 6 well plates were purchased from VWR. Acetone and *n*-heptane were purchased from Sigma. EDC activation buffer was prepared from 0.1 M MES buffer and 0.5 M NaCl solution. The deionized (DI) water that was used for all experiments (Millipore Corp. MilliQ system) had a specific resistance greater than 1 MΩ·cm (i.e., "equilibrium water"). Silicon wafers with an orientation of ⟨1-0-0⟩ and resistivity values of 1−10 Ω·cm, used as the substrate for FESEM imaging, were purchased from Silicon Quest International (lot IMV3P01-10PRM).

Equipment. The ultrasonicator was from VWR International (model 550T). The confocal and DIC optical microscopic images were obtained on an Olympus Fluoview 300 confocal laser scanning microscope at the Huck Institute of the Life Sciences Center for Quantitative Cell Analysis. The electron microscopic images were obtained on a ZeissSMT 1530 field emission scanning electron microscope (FESEM) at the Penn State Nanofabrication Facility. The pressurized heat treatments took place in a standard steam autoclave at 120 °C.

Preparation of Imaging Particles. Sulfate-functionalized fluorescent nile red (or yellow-green) PSL particles (4.0 μm, 200 μL) were encapsulated with 20 μM PAH in 30 mM KCl via layer-by-layer (LbL) assembly in a 50 mL centrifuge tube. The solution of particles and PAH was well dispersed with 5 min of sonication. For electrostatic adsorption, the particles in PAH solution were then incubated on a shaker plate (low speed) for 20 min. The PAH-coated particles were then centrifuged out of solution into a pellet at 6500 rpm for 30 min in a standard bucket centrifuge. The supernatant was removed with a plastic pipet and the PAH-coated particles were resuspended in 10 mL of 30 mM KCl. This centrifugation/resuspension process was repeated twice with the final resuspension being in 40 mL of deionized (DI) water. From this final solution, 10 mL of the final solution was placed in each of four small plastic Petri dishes that contained a piranha-etched (3:1 ratio of sulfuric acid to hydrogen peroxide) glass coverslip. The PAH-coated particles in DI water were left for 24 h to settle and electrostatically adhere to the negatively charged glass surface of the glass coverslip. Next, the coverslip was washed 20 times with approximately 10 mL of DI water to remove any excess or unadhered PAH-coated particles from the solution. An additional 20 mL of DI water was then added to the plastic Petri dish for storage of the PAH-coated sulfate-functionalized fluorescent particles until they were to be modified for creation of the multifunctional assembly.

Surface Modification with RGD or RAD: *RGD/RAD Modification via Particle Lithography (Type I).* Carbodiimide chemistry was performed for chemical modification of the PAH-coated PSL particles with peptides. In the first step, 2 mL of 10 μg/mL protein (GRGDSP or GRADSP) was added to a solution consisting of 2 mL of 5 mM NHS and 2 mL of 2 mM EDC in a 15 mL centrifuge tube. The solution was then incubated on a shaker plate (low setting) for 15 min at room temperature. During this time, the PAH-coated PSL particles adhered to the glass coverslip were washed with 10 mL of EDC activation buffer and were left to sit for 10 min at room temperature. After 15 min, 3 μL of 20 mM 2-mercaptoethanol was added to the protein solution to quench the reaction. Next, the protein solution was incubated (low setting) with the PAH-coated PSL particles adhered to the glass coverslip in 10 mL of EDC activation buffer for 2 h at room temperature. Here the peptide was being covalently bound to the PAH coating on the imaging particles in all areas except where the imaging particles were masked off by being adhered to the glass surface. After 2 h, the reaction was quenched by adding 2 mL of 10 mM hydroxylamine in EDC activation buffer (pH 6.0). Next, the RGD/RAD-modified particles stuck to the glass surface were rinsed with DI water 10 times. In the last rinse step, 10 mL of 100 mM PBS buffer (pH 7.4) was added to the particles and the samples were refrigerated for later use.

RGD/RAD Modification in the Lithographed Region (Type II). We took a plastic Petri dish of prepared imaging particles (on a glass coverslip surface) and poured off the DI water. We then added 10 mL of 30 mM KCl solution to the Petri dish. Next, we added 5 μL of 190 nm sulfate-functionalized fluorescent yellow-green (or nile red) PSL nanoparticles and dispersed the particles evenly with gentle agitation to the Petri dish. We waited 24 h to allow the nanoparticles to settle and electrostatically adhere to the PAH-coated imaging particle surfaces in all areas except where the imaging particles were masked off by being adhered to the glass surface.[23] Next, the imaging particles were washed 20 times to remove any excess or unadhered nanoparticles from the solution. An additional 10 mL of DI water was added to the Petri dish and the solution was placed in the autoclave for 10 min at 120 °C. At this temperature the PSL imaging particles start to soften and better affix the nanoparticles to the surface of the imaging particles. Once the pressurized heating process was complete, the nanoparticles were permanently fused to the surface of the imaging particles.[24] The glass coverslip was then washed 10 times to remove any particles that may have detached during the fusing process. Finally, 10 mL of EDC activation buffer was added to the particles (adhered to the glass surface). The nanoparticle-lithographed PSL imaging particles were then sonicated off the glass surface by placing the coverslip in a plastic Petri dish in the ultrasonicator for 15 s. The solution of lithographed

particles in EDC activation buffer was then placed in a 50 mL centrifuge tube and left to sit for 10 min.

Carbodiimide chemistry was then performed for chemical modification of the nanoparticle- and PAH-coated PSL particles with peptides. In the first step, 2 mL of 10 μg/mL protein (GRGDSP or GRADSP) was added to a solution consisting of 2 mL of 5 mM NHS and 2 mL of 2 mM EDC in a 15 mL centrifuge tube. The solution was then incubated on a shaker plate (low speed) for 15 min at room temperature. During this time, the PAH-coated PSL particles adhered to the glass coverslip were washed with 10 mL of EDC activation buffer and were left to sit for 10 min at room temperature. After 15 min, 3 μL of 20 mM 2-mercaptoethanol was added to the protein solution to quench the reaction. Next, the protein solution was incubated (low setting) with the nanoparticle-lithographed PSL imaging particles in EDC activation buffer for 2 h at room temperature. Here the RGD/RAD was being covalently bound to the PAH coating on the imaging particles in the lithographed region, which was the area that does not contain nanoparticles and was masked off during the nanoparticle coating process. After 2 h, the reaction was quenched by adding 2 mL of 10 mM hydroxylamine in EDC activation buffer (pH 6.00). Next, the RGD/RAD-modified nanoparticle-coated PSL imaging particles were rinsed by centrifugation. The solution was centrifuged at 5000 rpm for 30 min. The supernatant was removed and the multifunctional assembly particles were redispersed in 5 mL of DI water. This process was repeated two times. After the last centrifugation step, the supernatant was removed and the multifunctional assembly particles were redispersed in 1 mL of 0.1 M PBS (pH 7.4) at 37 °C. The multifunctional carrier assembly particle solution was stored in the refrigerator until further use.

FESEM Particle Sample Preparation. Approximately 2-μL particle assembly samples (<0.01% solids) were atomized onto a silicon wafer and left to air-dry. FESEM images were taken at a gun power of 1−2 kV and working distances between 3 and 6 mm.

Cell Culture. Murine NIH/Swiss 3T3 mouse fibroblast cells (ATCC, CRL-1658) were cultured at 37 °C in 5% CO_2 incubator with growth medium containing 89% DMEM, 10% FBS, and 1% antibiotic. Cells cultured in T-75 flasks were subcultured at a seeding density of 5×10^5 cells/mL (subconfluence) into a single well of a six-well plate. Cells used for imaging were grown on 25 mm glass coverslips (VWR) or 25 mm silicon wafer pieces. Glass coverslips were autoclaved and placed at the bottom of a single well of a six-well plate. The silicon wafer pieces were piranha-etched, autoclaved, oxygen plasma-cleaned, and placed at the bottom of a single well of a six-well plate. Each well contained 2.0 mL of medium. Cells were plated 1 day before experiments to allow for cell attachment and spreading.

Cell Adhesion Assay (Type I). The 3T3 cells were split onto glass coverslips that contained electrostatically adsorbed sulfate-functionalized PSL particles. The surface of the PAH-coated PSL particles was covalently modified with RGD or RAD by EDC chemistry. The 3T3 cells were incubated with the particles for 24 and 48 h to allow for cell attachment, spreading, and growth. Adhesion of 3T3 cells to lithographed RGD or RAD molecules on the surface of the PSL particles was evaluated by confocal microscopy. Cells were fixed with 3.75% paraformaldehyde and stained with appropriate dyes for imaging. Alexa Fluor-568 phalloidin (Molecular Probes) was utilized for F-actin visualization and DRAQ5 was utilized for nucleus imaging. The samples were mounted on glass slides by use of Prolong antifade solution (Molecular Probes). The preparations were then visualized with confocal microscopy.

Cell Adhesion Assay (Type II). The 3T3 cells were subcultured onto glass coverslips (and/or oxygen plasma-cleaned silicon wafer pieces) in six-well plates. All medium was removed, and 200 μL of multifunctional assembly particles in 100 mM PBS was added to the center of the glass coverslip (silicon wafer). An additional 2 mL of medium was added to the center of each glass coverslip. The samples were incubated for 24- and 48-h assays before imaging for adhesion of the RGD/RAD-modified lithographed region to the 3T3 cells with

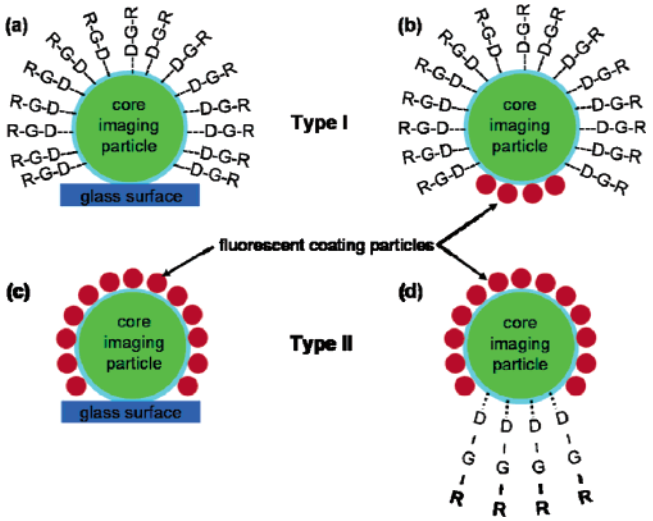

Figure 1. Schematic of type I and II classes of multifunctional carriers. (a) An imaging particle (green) is coated by the particle lithography technique with targeting ligands (RGD) with a glass substrate for type I assembly. (b) The modified imaging particle is sonicated off the glass substrate surface, and the lithographed region contains electrostatically adsorbed fluorescent nanoparticles (red). (c) An imaging particle (green) is coated by the particle lithography technique with fluorescent red nanoparticles with a glass substrate for type II assembly. (d) The coated imaging particle is sonicated off the glass substrate surface, and the lithographed region is covalently modified with targeting ligands (RGD). The thin layer of blue coating around the core imaging particle represents a polyelectrolyte layer coating.

FESEM. Cells were fixed with 2.5% glutaraldehyde in 0.2 M cacodylate buffer (pH 7.2) and buffer-washed three times with 0.1 M cacodylate buffer (pH 7.2). Cells underwent a secondary fixation with 1% osmium tetroxide in 0.1 M cacodylate buffer and were buffer-washed three times with 0.1 M cacodylate buffer. Samples were then dehydrated through a gradient series of ethanol [25%, 50%, 70%, 85%, 95%, and 100% (three times)] for 5 min at room temperature. The samples were then dried at their critical point with bone-dry liquid carbon dioxide ($4 \times$ 3-min exchanges plus an 8-min vent). The samples were then visualized with FESEM.

Results and Discussion

Fabrication of a Multifunctional Vector. The particle lithography technique[23] was applied to create two classes of multifunctional precursor carriers in order to demonstrate localized targeting by use of the RGD peptide sequence for an in vitro 3T3 cell culture model. Particle lithography is a technique that consists of adhering particles to a surface, such that the surface masks the contact point of the particle and the surface. When polyelectrolytes or nanoparticles (or small molecules) are introduced, they adsorb over the entire particle except where the surface masks the particle at the contact point. The first class of carriers, type I, is schematically shown in Figure 1a,b, where ~98% of the surface of the imaging particle is chemically modified by the particle lithography technique with RGD peptide targeting ligands and the lithographed region contains electrostatically adhered fluorescent nanoparticles. The second class of carriers, type II (Figure 1c,d), is the complement to type I, such that the lithographed region is chemically modified with the RGD peptide sequence, and the rest of the particle is coated with electrostatically adhered fluorescent nanoparticles.

Figure 2 shows an FESEM image of a precursor to the assembly in Figure 1b of 3.0 μm silica particles coated with 84

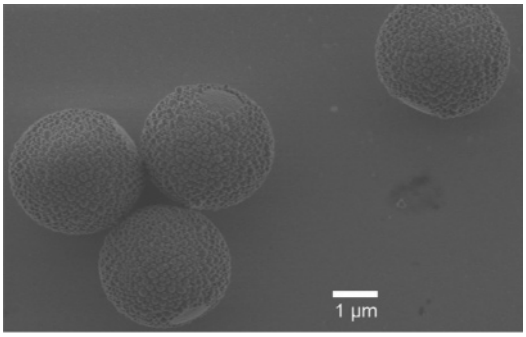

Figure 2. FESEM image of 3 μm lithographed silica particles. Silica particles were coated with PAH and then the particle lithography technique was performed with 84 nm sulfate-functionalized nanoparticles in an ionic strength of 30 mM KCl. Diameter of the lithographed regions is approximately 960 nm.

nm sulfate-functionalized PSL nanoparticles by the particle lithography technique[23] in an ionic strength of 30 mM KCl. The diameter of the lithographed regions is approximately 960 nm, which closely matches the value of 1000 nm that is predicted from a simple geometric calculation.[23,25]

Both type I and type II classes of multifunctional carriers are envisioned to be essential developments for focused drug delivery and diseased tissue imaging. The main objective of this work was to illustrate the robustness of this inexpensive technique for assembling colloidal carriers with multifunctional regions. Layer-by-layer assembly can be applied at any point during the particle lithography process. For example, the core fluorescent PSL imaging particles can be coated with cationic polyelectrolytes to provide an appropriate surface for chemical modification with targeting ligands. The nanoscale precision and control over the diameter of the lithographed region has been previously shown with FESEM analysis (Figure 2).[25]

We used fluorescent confocal microscopy to demonstrate the presence of the lithographed region on the surface of the core imaging PSL particle. Confocal microscopy with a high numerical aperture objective (NA = 1.3) has a spatial resolution of ~200 nm and is relatively straightforward to use. PAH-coated, sulfate-functionalized, fluorescent nile red particles (4.0 μm) were coated with 160 nm sulfate-functionalized fluorescent yellow-green particles by the particle lithography technique to create type II carriers. This assembly was fabricated on a flat glass coverslip surface and fused for 15 min in a standard steam autoclave before being imaged with confocal microscopy. The particle assemblies remained attached to the glass coverslip for ease of imaging, such that the microscope objective images directly through the glass substrate where the lithographed patch is adhered. The images in Figure 3 demonstrate that the core and coating particles remain fluorescent and electrostatically adhered to the glass surface. This observation is important because it supports the fact that the particle lithography process does not alter the chemical properties of the nanoparticles or imaging particles. Since the particle assemblies were still adhered to the glass coverslip surface, we could easily visualize the presence of the lithographed region as the light red fluorescent core of the particle. The fluorescent image in Figure 3d shows the lithographed region with a patch size of approximately 1.5 μm.

A similar assembly to that shown in Figure 3 was imaged with a three-dimensional analysis by use of *z*-stacking in confocal microscopy. The image seen in Figure 4 shows a confocal microscopy overlap image (red and green laser excitations) at a height of 8 μm in the sample of 4 μm sulfate-functionalized fluorescent nile red particles PAH-coated and

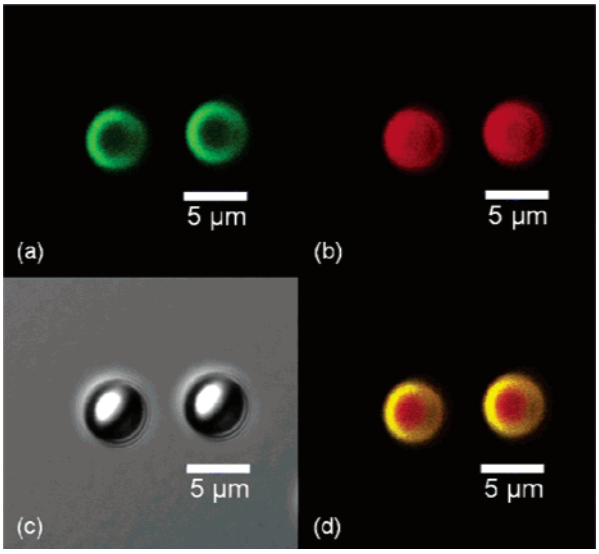

Figure 3. Confocal microscopic image at 60× oil magnification of a 4 μm sulfate-functionalized fluorescent nile red particle PAH-coated and lithographed with 190 nm sulfate-functionalized fluorescent yellow-green nanoparticles. Image of the lithographed particle assembly excited with (a) the blue laser and (b) the green laser are shown, along with (c) the DIC image and (d) an overlap of images a and b.

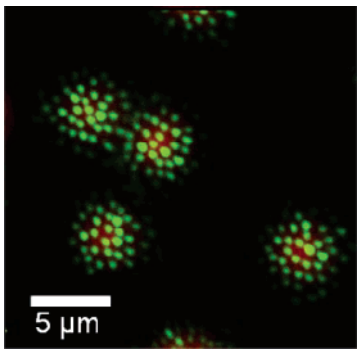

Figure 4. Confocal microscopic image at 60× oil magnification of 4 μm sulfate-functionalized, fluorescent nile red particles PAH-coated and lithographed with 190 nm sulfate-functionalized fluorescent yellow-green nanoparticles. The image of the lithographed particle assembly is excited with the blue and green lasers.

lithographed with 190 nm sulfate-functionalized, fluorescent yellow-green nanoparticles in deionized water. The individual 190 nm sulfate-functionalized fluorescent yellow-green nanoparticles are clearly visible on the surface of the core fluorescent nile red particles. Each individual nanoparticle was able to be observed because the *z*-stack image was taken above the top of the particle assemblies and because the assemblies were not autoclaved, such that the individual nanoparticles adhered to the core particle surface remained separated and did not fuse together to make a more uniform coating layer. If the assemblies were fused, then the *z*-stack image taken from above the assemblies would show the surface appearing as a slightly blurred green color.

A precursor similar to the type I assembly was created by use of 4.0 μm sulfate-functionalized PAH-coated PSL imaging particles lithographed with 200 nm sulfate-functionalized nanoparticles and electrostatically adhered in the lithographed region with 43 nm carboxyl-functionalized fluorescent orange nanoparticles. This assembly was imaged by confocal microscopy, and the lithographed region can be clearly seen as the fluorescent red patch in Figure 5b,c. In addition, the flattened lithographed region is visible in the DIC image as marked by the arrow. The

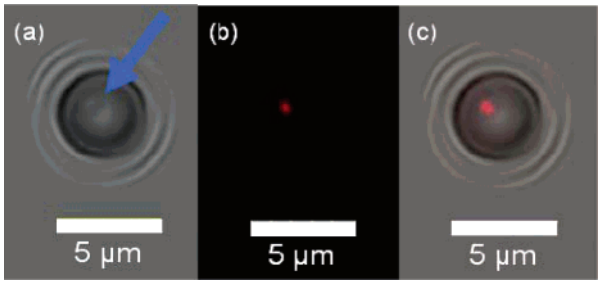

Figure 5. Confocal microscopic image of a type I assembly consisting of a 4.0 μm sulfate-functionalized, PAH-coated PSL imaging particle lithographed with 43 nm sulfate-functionalized nanoparticles and 200 nm carboxyl-functionalized fluorescent orange nanoparticles that were electrostatically adhered in the lithographed region. Images of the type I particle assembly are shown: (a) DIC showing a subtle flattened lithographed region to the upper left of the particle center, marked by the blue arrow; (b) excitation with the green laser; and (c) overlay of images a and b. Similar images were taken with multiple samples.

fluorescent particles adhered to the lithographed region appear as a single fluorescent patch because the multiple nanoparticles are tightly packed from being adhered in an ionic strength of 30 mM KCl. On the basis of the fluorescent patch, the size of the lithographed region was estimated to be 1000 nm, which is in agreement with the FESEM and confocal microscopic results from Figures 2 and 3.

The results from confocal microscopy and FESEM confirm the presence of a lithographed region fabricated by the particle lithography technique. The size of the lithographed region patch can be estimated by confocal microscopy and accurately sized by FESEM. After the multifunctional carrier had been fabricated, the next step involved chemical modification of the lithographed and nonlithographed regions with targeting ligands for the type I and II colloidal carrier assemblies, as well as showing the assembly's specificity with cell adhesion assays.

Ligand-Specific Interactions by RGD Peptide-Modified PAH-Coated Particles. A 3T3 fibroblast cell line was chosen as a model system to investigate the interaction between the integrin $\alpha_v\beta_3$ cell surface receptors with RGD-modified lithographed particles. This 3T3 fibroblast cell line has been commonly used in the literature to study integrin-mediated cell adhesion to RGD peptide-modified surfaces.[17,26−28] In this study, it was hypothesized that the covalent attachment of RGD to the nonlithographed or lithographed regions on the multifunctional carrier would promote integrin-mediated cell adhesion and spreading. To test this hypothesis, peptides containing the RGD and RAD motifs were covalently coupled to the PAH-coated surfaces of type I and II multifunctional carriers through the use of carbodiimide chemistry. The RAD motif gives a nonspecific variation in the integrin binding site and serves as a control to the strongly adhering RGD motif for the inhibition of cell attachment and spreading.

Type I Assembly Adhesion Assay. The first studies performed were 24- and 48-h cell adhesion assays in which 3T3 fibroblast cells were incubated on glass coverslips containing RGD- or RAD-modified lithographed particles (fluorescent yellow-green) electrostatically adhered to the glass coverslip surface. The ligand-modified core imaging particles were randomly distributed at an area fraction of ~25%. After incubation, the cells were rinsed a minimum of four times with 0.1 M PBS at 37 °C, fixed, and stained for visualization of the actin filaments and the nucleus. Figure 6 summarizes the confocal microscopic results for 24- and 48-h adhesion assays with RGD and RAD modifications. After 24 and 48 h, the 3T3 cells have adhered to the RGD- and RAD-modified particles and spread.

After 24 h, on average the 3T3 cells had adhered to 30 ± 11 ($n = 5$) RGD-modified lithographed particles, which were adhered to the glass substrate. In order to determine whether the cells remained attached to the particle surface or if the cells had endocytosed the particles, a three-dimensional analysis using *z*-stacking with confocal microscopy was used. Figure 6a represents the middle slice of an *xyz* image for the 24-h adhesion assay study. The yellow cross hairs indicate the position of the *xz* and *yz* slices, which are located to the right and on the bottom of Figure 6a, respectively. The slices show that the cells are attached to the focal points on the imaging particle surface, and thus it is not a purely focusing adjustment that alters the position of the particles compared to that of the cells. The *xz* and *yz* slices indicate that the imaging particles are not located in the same plane as the nucleus/actin cytoskeleton and thus remain adhered to the cell *surface* via integrin−RGD interactions and were not taken up within the cell. The actin cytoskeleton (red) illustrates that the cellular membrane has spread upon adhesion to the RGD-modified lithographed imaging particles.

After 48 h of incubation, the 3T3 cells have internalized the RGD-modified lithographed particles via receptor-mediated endocytosis. Figure 6b *xz* and *yz* sliced images show that the actin cytoskeleton (red) surrounds the RGD-modified particles (green) and the particles are within the same plane as the nucleus. Schraa et al.[29] have also demonstrated in vitro receptor-mediated endocytosis of RGD-modified proteins incubated with human primary umbilical vein $\alpha_v\beta_5$ integrin receptor expressing endothelial cells. The combined 24- and 48-h RGD adhesion study results indicate that our multifunctional carrier assembly can specifically adhere to the cell surface via receptor−ligand interactions and be successfully internalized within the cells. The fact that the particles had a single nanoscale region that had no RGD modification is not important at this point.

Integrins exist in different affinity states with respect to their ligands and can enter a high-affinity state or activated state in response to an agent.[30] As expected, the 3T3 fibroblast cells bound successfully to the RGD motif modified on the surface of the imaging particles that were electrostatically adhered to the glass coverslip surface. Upon binding, the integrin receptors were likely activated and thus initiated adhesion and plasma membrane spreading (branched cytoplasm). The observed cell attachment and spreading after 24 h suggests that the RGD activity was retained after chemical coupling to the imaging particle. This adhesion and spreading was also observed to be independent of the number of particle assemblies available for binding. The cell adhesion and spreading resulted in the particle assemblies clustering together. In addition, it was observed that a minimum of two particle assemblies was required for cell adhesion and spreading to occur. Similar observations were made by Maheshwari et al.,[31] and they demonstrated that integrin clustering is essential to support cell adhesion and motility. Our in vitro studies show that RGD-modified multifunctional carrier particles specifically bind to integrin receptors expressed on 3T3 cells.

Although the 3T3 fibroblast cells adhered to the RAD-modified lithographed particles, the cell response was different from that of the RGD modification. After 24 and 48 h of incubation, the actin cytoskeleton continued to grow and the cells remained alive. To again determine whether the cells were attached to the particle surface or taken up into the cell, confocal microscopy three-dimensional *z*-stacking was used. Figure 6 panels c and d represent bottom slices (near the glass coverslip substrate surface) of *xyz* images for the 24- and 48-h RAD adhesion assay studies. The yellow cross hairs show the position

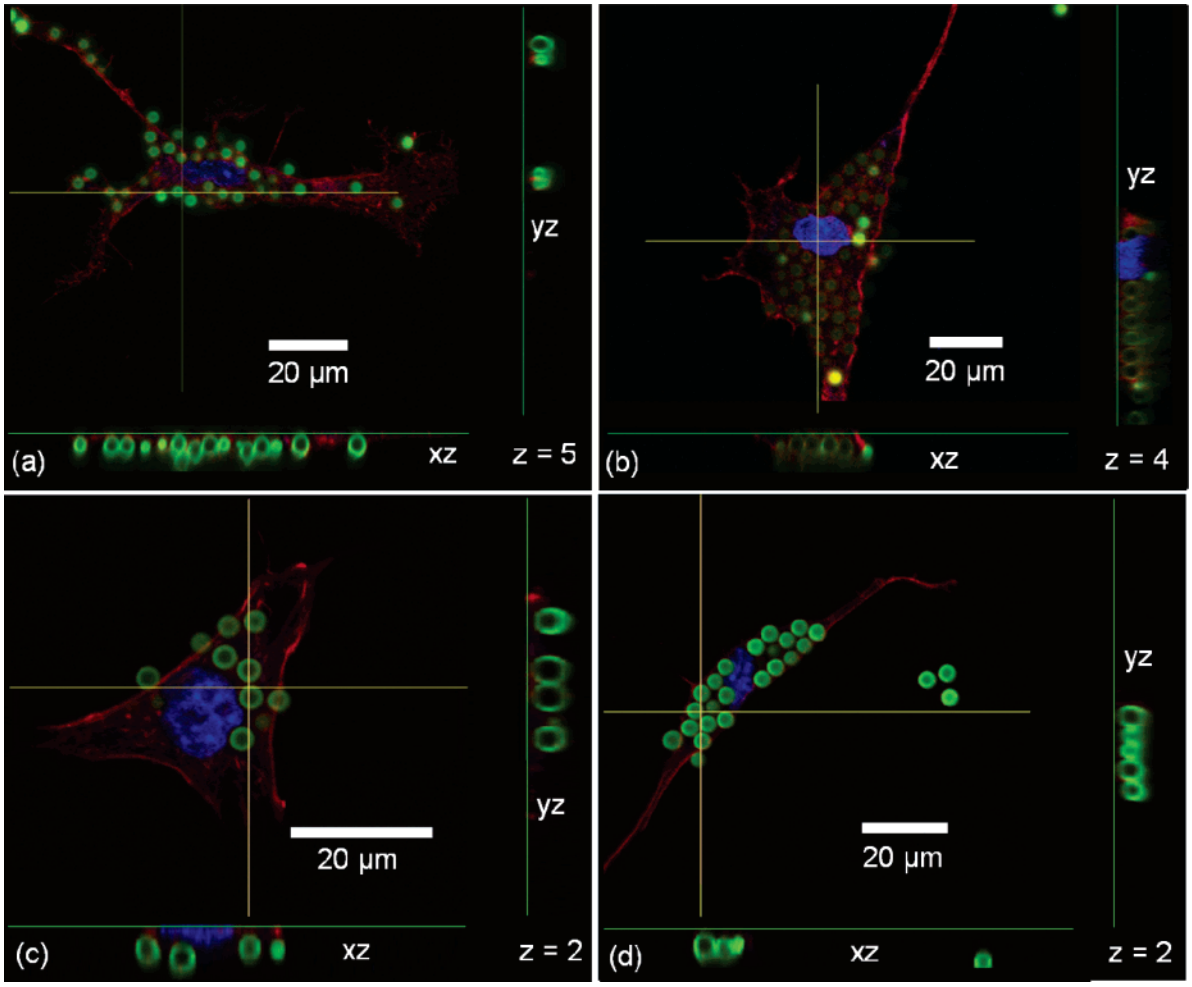

Figure 6. Confocal microscopic images of 3T3 fibroblast cells adhered to RGD- and RAD-motif lithographed 4 μm sulfate-functionalized PSL fluorescent yellow-green particles assembled on glass coverslips. After 48 h the RGD-motif modified imaging particles were taken up into the 3T3 cells. (a) 24-h RGD-motif assay *xyz* image from *z*-stack taken from the middle slice. (b) 48-h RGD-motif assay *xyz* image from *z*-stack taken from the middle slice. Note that the particles were taken up into the cell. (c) 24-h RAD-motif assay *xyz* image from *z*-stack taken from a bottom slice. (d) 48-h RAD-motif assay *xyz* image from *z*-stack taken from a bottom slice. The cross-hairs identify the position of *xz* and *yz* planes, and the images were taken at 60× with oil. The cell actin cytoskeleton was stained red with Alexa 568 phalloidin, the nucleus was stained blue with DRAQ5, and the particles were fluorescent yellow-green.

of the *xz* and *yz* slices, which are located to the right and on the bottom of Figure 6c,d, respectively. The *xz* and *yz* slices show that the RAD-modified imaging particles are clearly located on a different plane than the nucleus and the actin cytoskeleton after 24 and 48 h in the adhesion assay. The RAD-modified particles may have been specifically or nonspecifically adhered to the cell surface, but receptor−ligand binding and integrin activation did not occur because the particles were not taken up within the cell. The *xz* and *yz* slices for the 48-h assay in Figure 6d show only the fluorescent green imaging particles and little or no red actin cytoskeleton, indicating that the cell may not be adhered to the particles that are adhered to the substrate surface since the particles and cell are on drastically different focal planes.

During imaging of the 24- and 48-h adhesion assays for RGD and RAD modifications, it was observed that RGD-modified particles were always found attached to or near a cell, whereas the RAD-modified particles were often found randomly dispersed on the substrate surface without any cells present. One hypothesis is that the nonspecific 3T3 cell adhesion to the RAD-motif lithographed imaging particles was mediated though electrostatic interactions. Another possible reason for adhesion is that protein in the serum medium may have aided nonspecific adhesion of the 3T3 fibroblast cells to the RAD-modified imaging particles by conditioning the surface of the modified particles with serum proteins and allowing the cells to stick by the usual cell growth mechanisms. It is known that the RGD peptide ligand binds at the interface between the αV and β3 subunits with contacts between the aspartic acid group and the β3 subunit, as well as contact between the arginine (cation) residue and the βA ligand-binding domain of the β3 subunit, which stabilizes the ligand-binding surface.[32] The glycine residue plays an important role in making hydrophobic interactions with the αV subunit while lying at the α and β subunit interface.[32] The single residue change to alanine for the RAD control modification does not provide the hydrophobic interactions to result in conformational correct binding and integrin activation of the cell.[33,34] Thus, we believe that the integrin receptors were not being activated upon binding to the RAD motif and receptor-mediated endocytosis did not occur.

Type II (Small Lithographed Region) Assembly Adhesion Assay. The second set of studies performed with the type II assembly was a 48-h cell adhesion assay in which the 3T3 fibroblast cells grown on silicon wafers were inoculated with imaging particles lithographed with 200 nm nanoparticles and modified with RGD or RAD motif only in the lithographed (bare patch) region. After 48 h, the assay samples were washed four times with 0.1 M PBS at 37 °C, fixed, dried in liquid CO_2, and

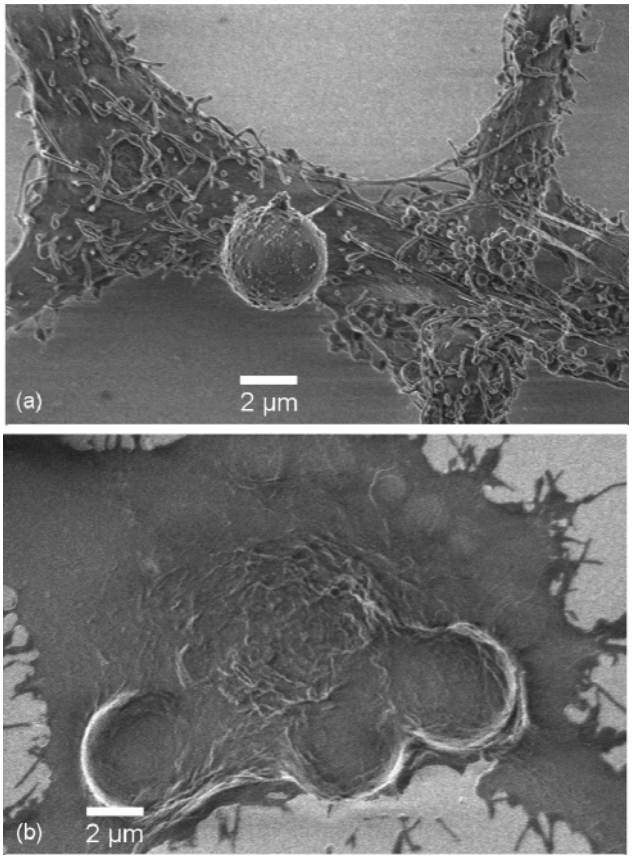

Figure 7. FESEM images of 48-h adhesion assay with 3T3 fibroblast cells and 4 μm sulfate-functionalized PAH-coated imaging particles lithographed with 200 nm sulfate-functionalized PSL particles and (a) RAD- or (b) RGD-motif modified in the lithographed region.

imaged with FESEM. Figure 7a illustrates that the RAD-modified lithographed region particle assemblies were nonspecifically adhered to the surface of the cells. The flattened lithographed regions (modified with RAD motif) are clearly visible in the images, indicating that receptor−ligand interactions did not occur. The presence of type II particle assemblies on the surface of the cells could be nonspecific from electrostatic interactions, part of the RAD peptide contacting the integrin receptor, as well as from surface tension present during the sample drying process. Figure 7b shows that the RGD-modified lithographed region particle assemblies specifically adhered to the cells and the actin cytoskeleton had grown over the assembly by receptor-mediated endocytosis. There was a distinct difference in the 3T3 fibroblast cell growth when RAD and RGD lithographed region modifications were made to the colloidal assemblies. When the RGD modification was used, the cells grew over the particles and appeared morphologically different, as was hypothesized from the confocal microscopy results. These FESEM images further validate the 48-h RGD adhesion assay (confocal microscopy receptor-mediated endocytosis results) for the type I assembly and clearly demonstrate the effectiveness of our multifunctional colloidal carrier scheme. If the particles were fully functionalized with RGD or RAD (i.e., particle lithography was not used during the functionalization process), then the same adhesion and uptake seen with the type I and II assemblies would occur.

Conclusions

The particle lithography technique has the ability to create site-specific chemical modifications on the surface of colloidal particles and nanoparticles and was utilized in this work to prepare a multifunctional targeting and imaging carrier assembly. The surface chemistry of the imaging particles in the lithographed and nonlithographed regions were controlled with nanoscale precision. Confocal microscopy and FESEM imaging analysis illustrate our successful fabrication of the type I and II multifunctional colloidal carriers. The lithographed or nonlithographed regions can be easily tailored to include electrostatically adhered fluorescent (or even drug) nanoparticles or targeting moieties covalently bound to the imaging particle surface. Applying the particle lithography technique has allowed for a unique fabrication process for a multitude of colloidal imaging carriers with multiple information regions.

In vitro results showed 3T3 fibroblast cells specifically adhering to clusters of RGD-motif lithographed imaging particles after 24 and 48 h of incubation. These in vitro results suggest that localized targeting to the surface cell integrins was accomplished. Endocytosis of the RGD-motif modified particles was observed with confocal microscopy after 48 h of incubation. A second set of studies, using the type II colloidal carrier with FESEM analysis, further demonstrated localized targeting to the surface cell integrins and endocytosis of the RGD-motif modified particles, as well as nonspecific adhesion of the RAD-motif modified particles resulting in morphologically different cytoplasm growth. From the FESEM images, it is clear that the 3T3 fibroblast cells displayed distinct morphological differences in their cytoplasm after nonspecific adhesion to the RAD motif modified on the imaging particles. The change in cell behavior was hypothesized to be a direct result of an inactive receptor−ligand interaction.

Our results demonstrate the capability of fabricating a multifunctional colloidal carrier with site-specific regions of chemical "information" through application of the particle lithography technique. It can be envisioned that the proposed multifunctional carriers have the potential to accomplish two tasks: (1) They can selectively image the cell surface or tumor endothelium, and (2) the carriers can actively target to deliver therapeutic agents, by addition of locally placed drug nanoparticles to a specific region on the colloidal carrier surface, to the endothelial cell via receptor-mediated endocytosis.

Acknowledgment. We thank the National Science Foundation (NIRT Grant CCR-0303976), the Petroleum Research Fund (Grant PRF 43453-AC10), and the Commonwealth of Pennsylvania for funding. We thank the Penn State Materials Research Institute for funding the FESEM images taken at the Penn State Nanofabrication Facility, part of the NNIN. We also thank the Huck Institute of Life Sciences Center for Qualitative Cell Analysis for their assistance and use of their Olympus Fluoview 300 confocal laser scanning microscope, as well as the Electron Microscopy Facility for their assistance with FESEM sample preparation.

References and Notes

(1) Allen, T. M.; Cullis, P. R. *Science* **2004**, *303*, 1818−1822.
(2) Feng, S.-S.; Chien, S. *Chem. Eng. Sci.* **2003**, *58*, 4087−4114.
(3) Sahoo, S. K.; Labhasetwar, V. *Drug Discovery Today* **2003**, *8*, 1112−1120.
(4) Shchukin, D. G.; Gorin, D. A.; Mohwald, H. *Langmuir* **2006**, *22* (17), 7400−7404.
(5) Langer, R. *Science* **1990**, *249*, 1527−1533.
(6) LaVan, D. A.; McGuire, T.; Langer, R. *Nat. Biotechnol.* **2003**, *21* (10), 1184−1191.
(7) Farokhzad, O. C.; Cheng, J.; Teply, B. A.; Sherifi, I.; Jon, S.; Kantoff, P. W.; Richie, J. P.; Langer, R. *Proc. Natl. Acad. Sci.* **2006**, *103*, 6315−6320.
(8) Ferrari, M. *Nat. Rev.* **2005**, *5*, 161−172.

(9) Liu, T. F.; Cohen, K. A.; Ramage, J. G.; Willingham, M. C.; Thorburn, A. M.; Frankel, A. E. *Cancer Res.* **2003**, *63*, 1834−1837.
(10) Leodore, L. M.; Lathia, J. D.; Wheatly, M. A. *Proc. 29th Annu. IEEE Bioeng. Conf.* **2003**, 193−194.
(11) Ku, G.; Wang, X.; Xie, X.; Stoica, G.; Wang, L. V. *Appl. Opt.* **2005**, *44* (5), 770−775.
(12) Li, L.; Wartchow, C. A.; Danthi, S. N.; Sheh, Z.; Dechene, N.; Pease, J.; Choi, H. S.; Doede, T.; Chu, P.; Ning, S.; Lee, D. Y.; Bednarski, M. D.; Knox, S. J. *Int. J. Radiat. Oncol. Biol. Phys.* **2004**, *58* (4), 1215−1227.
(13) Dirks, P. B. *Nature* **2006**, *444*, 687−688.
(14) Morabito, A.; Sarmiento, R.; Bonginelli, P.; Gasparini, G. *Crit. Rev. Oncol. Hematol.* **2004**, *49*, 91−107.
(15) Arap, W.; Pasqualini, R.; Ruoslahti, E. *Science* **1998**, *279*, 377−380.
(16) Ruoslahti, E. *Annu. Rev. Cell Dev. Biol.* **1996**, *12*, 697−715.
(17) Shu, X. Z.; Ghosh, K.; Liu, Y.; Palumbo, F. S.; Luo, Y.; Clark, R. A.; Prestwich, G. D. *J. Biomed. Mater. Res. A.* **2004**, *68*, 365−375.
(18) Mardilovich, A.; Craig, J. A.; McCammon, M. Q.; Garg, A.; Kokkoli, E. *Langmuir* **2006**, *22*, 3259−3264.
(19) Zahr, A. S.; deVilliers, M.; Pishko, M. V. *Langmuir* **2005**, *21* (1), 403−410.
(20) Lvov, Y.; Decher, G.; Möhwald, H. *Langmuir* **1993**, *9*, 481−486.
(21) Shenoy, D. B.; Antipov, A. A.; Sukhorukov, G. B.; Mohwald, H. *Biomacromolecules* **2003**, *4*, 265−272.
(22) Decher, G. *Science* **1997**, *277*, 1232−1237.
(23) Snyder, C. E.; Yake, A. M.; Feick, J. D.; Velegol, D. *Langmuir* **2005**, *21* (11), 4813−4815.
(24) Yake, A. M.; Panella, R. A.; Snyder, C. E.; Velegol, D. *Langmuir* **2006**, *22*, 9135−9141.
(25) Yake, A. M.; Snyder, C. E.; Velegol, D. Site-Specific Functionalization on Individual Colloids: Size Control, Stability and Multi-Layers. Submitted for publication 2007.
(26) Hynes, R. O. *Cell* **1992**, *69*, 11−25.
(27) Dai, W.; Saltzman, W. M. *Biotechnol. Bioeng.* **1996**, *50*, 349−356.
(28) Krishna, G.; Shutava, T.; Lvov, Y. M. *Chem. Commun.* **2005**, *14*, 2796−2798.
(29) Schraa, A. J.; Kok, R. J.; Berendsen, A. D.; Moorlag, H. E.; Bos, E. J.; Meijer, D. K. F.; deLeij, L. F. M. H.; Molema, G. *J. Controlled Release* **2002**, *83*, 241−251.
(30) Aplin, A. E.; Howe, A.; Alahari, S. K.; Juliano, R. L. *Phamacol. Rev.* **1998**, *50*, 199−252.
(31) Maheshwari, G.; Brown, G.; Lauffenburger, D. A.; Wells, A.; Griffith, L. G. *J. Cell Sci.* **2000**, *113*, 1677−1686.
(32) Xiong, J.-P.; Stehle, T.; Zhang, R.; Joachimiak, A.; Frech, M.; Goodman, S. L.; Arnaout, M. A. *Science* **2002**, *296*, 151−155.
(33) Pierschbacher, M. D.; Ruoslahti, E. *Proc. Natl. Acad. Sci.* **1984**, *81*, 5985−5988.
(34) Hays, E. D. *Cell Biology of Extracellular Matrix*, 2nd ed.; Plenum: New York, 1991; p 347.

BM070071R